Effects of heating rate and metal binder on the microstructure and mechanical properties of self-diffusion gradient cermet composite tool materials

Wenbin Ji [a, b], Bin Zou [a, b, *], Chuanzhen Huang [a, b], Jun Wang [a, b], Kaitao Xu [a, b], Yanan Liu [a, b], Changming Huang [a, b]

[a] Centre for Advanced Jet Engineering Technologies (CaJET), School of Mechanical Engineering, Shandong University, Jinan 250061, PR China
[b] Key Laboratory of High Efficiency and Clean Mechanical Manufacture, Shandong University, Ministry of Education, PR China

ARTICLE INFO

ABSTRACT

Self-diffusion gradient cermet composite tool materials with different metal binder contents and Ni/(Co + Ni) mass ratios were fabricated to improve the mechanical properties. The effects of heating rate and metal binder on the microstructure and mechanical properties of self-diffusion gradient composite were investigated. For the heating rates considered, it was revealed that the heating rate of 30 °C/min was in the vicinity of optimum to yield the desired mechanical properties and fine microstructure. It was found that the flexural strength increased and the hardness decreased with increasing Ni binder content, while the addition of Co binder led to an excessively thick rim phase which was detrimental to the flexural strength. Applying a proper amount of Ni binder appeared to be beneficial for fabricating gradient composites with desired self-diffusion process during sintering. For the experimental conditions considered in this study, the best mechanical properties can be obtained when 6 mass% Ni in the surface and 12 mass% Ni in the substrate were used, which gave flexural strength, substrate hardness and surface hardness at 1488 ± 190 MPa, 20.96 ± 0.30 GPa and 25.12 ± 0.48 GPa, respectively.

1. Introduction

Increasing industrial needs for more efficient cutting of modern materials and higher reliability of tool performance give strong incentives for developing new tool materials. Cutting tools are requested to possess high strength, high hot hardness, and good wear and oxidation resistance [1]. However, it has always been a challenge to improve the flexural strength and hardness of materials simultaneously. Function gradient composites provide a good approach for the tool material to obtain the high flexural strength and hardness at the same time, so does cutting tool surface coatings. Cemented carbide cutting tools coated by physical vapor deposition (PVD) or chemical vapor deposition (CVD) technology exhibits high surface hardness and excellent wear resistance [2]. However, the coating of cutting tools can be worn off quickly in a machining of difficult-to-machine materials.

Hardmetals based on Ti(C,N) have been used as cutting tool materials due to their high edge strength, good wear resistance and high reliability [3]. Compared to the conventional WC-based hardmetals, Ti(C,N)-based cermets provide improved surface finish, excellent chip and tolerance and geometric accuracy control on workpieces, in addition to the ability to increase the cutting feeding speed [4]. Furthermore, Ti(C,N)-based cermets are much competitive in manufacturing costs and cutting performance compared to the WC-based hardmetals. Although the strength, hardness and toughness can be changed by varying the chemical compositions and fabrication parameters, an increase in the flexural strength and toughness is normally associated with a decrease in the hardness of cermet composites, and vice versa. For example, Liu et al. [5] fabricated a Ti(C,N)-based cermet with a high bending strength of 2210 MPa and a high toughness of 10.1 MPa m$^{1/2}$, but its HV hardness was as low as 14.7 GPa. TiB$_2$ ceramic is recognized as one of the best candidates for cutting tool materials owing to its low friction coefficient, high hot hardness and low adhesion with steel at the high temperatures [6]. However, TiB$_2$ exhibits a poor sintering ability due to the relatively low self-diffusion coefficient and

* Corresponding author. Shandong University, 17923 Jing Shi Road, Jinan 250061, PR China.
  E-mail address: zou20011110@163.com (B. Zou).

predominant covalent bonding. Therefore, some ceramic sintering additives such as TiC [7], VC [8] and SiC [9] are added into TiB_2-based composites to enhance their density and cutting performance. Vallauri et al. [10] reported that the favorable coherency between (111) TiC and (0001) TiB_2 interfaces contributed to the toughness of TiC—TiB_2 composite materials. Zou et al. [8] found that the hardness of TiB_2—TiC + Al_2O_3 composite was increased by the addition of 3.2 mass% superfine VC due to the homogenous microstructure with refined grains.

Material density, structure and mechanical properties are sensitive to the sintering process and metal binder additions [11]. In general, metal additives such as Ni [12], Co [13] and Mo [14] are used in the cermet composites to improve the sinterability, lower the sintering temperature and enhance the mechanical properties of the composites. In most Ti(C,N)-based cermets, the binder phase is mainly composed of Ni or Co, and the solid solution hardening of the binder phase plays a vital role in the performance of cermets [4]. Davies et al. [15] indicated that Ni was a preferred binder composition for TiC + TiB_2 composites. Conforto et al. [16] pointed out that a heavily disordered zone in the nanometric scale was observed at close to the interface with the core of Ti(C,N) grains in sintered samples. This disorder was correlated with the presence of Mo in the rim during sintering, which enhanced the strength of the core—rim interface as a barrier for the diffusion of atoms from the core. Zhang et al. [17] found that the ceramic grain of ultra-fine Ti(C,N)-based cermet becomes finer with the increase of Mo addition. They indicated that Mo improved the wettability between ceramic phase and metallic phase, decreased the solubility of Ti(C,N) in the binder and inhibited the grain growth during the liquid sintering stage. The metal binder redistributes under the high temperature, high pressure conditions during sintering leading to a remarkable variations of mechanical properties. Furthermore, the sintering conditions and the alloy status of metal binder after the sintering process affect the cutting performance of the composites [3]. Rajabi et al. [18] showed that an increase in sintering temperature to just above 1430 °C resulted in the decomposition of TiN and the formation of porosities. The decomposition of TiN fosters the decrease in mechanical proprieties of TiC-based cermet. Wang et al. [19] pointed out that quick hot pressing sintering at high temperature is the best sintering process for TiB_2 ceramic (short sintering time and high temperature) as long sintering times are responsible for grain growth. Numerous studies [19,20] have been conducted to obtain cermets with good microstructure and mechanical properties by optimizing the sintering temperature and holding time. However, little study on the effects of heating rate on the microstructure and mechanical properties of cermets have been reported, so does the effects of metal binder for the fabrication of self-diffusion gradient composites.

In this work, self-diffusion gradient composites are fabricated with different metal binder contents and Ni/(Co + Ni) mass ratios at different sintering heating rates. The mechanical properties are then investigated with a view to understand how these variables affect the material microstructure and the enhanced mechanical properties.

2. Material design and experimental work

The objective of the material design is to enhance the flexural strength, surface and substrate hardness of the composites by varying the composition contents and sintering parameters. It is well known [21] that, compounds containing the carbon and boron elements can be used as the surface of cutting tool materials; likewise, compounds containing the titanium and tungsten elements are suitable as the cutting tool substrate materials. In addition, there is a favorable compatibility between TiB_2—TiC and Ti(C,N). Therefore, the composite materials to be fabricated in this study are comprised of a TiB_2—TiC surface layer with good hardness and Ti(C,N)-based cermet substrate with good strength and toughness. After sintering, a new subsurface layer with metal binder enrichment is formed by a self-diffusion driving force of the elements. According to an earlier study [22], it is expected that the composites so fabricated will possess gradient properties with a high hardness and good wear-resistance on the surface layer, and a good flexural strength on the substrate. The subsurface layer with metal binder enrichment should have a good toughness and improved the interface bonding strength between the surface layer and substrate. In combining the self-diffusion characteristic during the sintering process and the gradient mechanical properties of the final materials, the composites so fabricated are termed as self-diffusion gradient composites. In addition, the composites in the present work also include Mo and VC additives to improve the sinterability and surface hardness of the composites.

The sintering temperature ranges usually from 1500 °C to 1700 °C for the TiB_2—Ni system [10], while from 1400 °C to 1500 °C for Ti(C,N)-based cermets [23]. The mismatches in the sintering temperature make the selection of this parameter difficult. According to our previous studies [24,25], Ti(C,N)-based cermet sintered at 1425—1475 °C exhibited the best mechanical properties. Moreover, TiB_2—TiC sintered at 1500—1550 °C by a vacuum hot-pressing sintering can yield fully dense microstructure. The wettability between metal binder and hard particles can be improved in a vacuum environment. The closure of pores and densification process can be accelerated at a high sintering pressure. In addition, the thickness of the TiB_2—TiC surface layer is designed at only 400 μm, so the content of TiB_2—TiC in the whole material is less than 10 mass%. Therefore, the 1475 °C sintering temperature is chosen to accommodate the two materials.

The actual sintering temperature of our sintering equipment changed from −3 to +3 °C, so the precise control of heating rate is difficult for our present sintering facility. Secondly, the preparation of cermets is not overly sensitive to the sintering temperature. In general, the increment of heating rate is 5 °C/min for cermet materials. Therefore, 20, 25, 30 and 35 °C/min are selected rationally for the self-diffusion gradient composites.

The mixtures of TiB_2—TiC powders (99.9% purity, 1.5 μm size) and Ti(C_7N_3) powders (99.9% purity, 0.5 μm size) were used as the starting materials. The average grain size of VC, Mo, Ni and Co powders used as sintering additives was 100—300 nm. The composition ratios of the starting composite materials are listed in Table 1. The self-diffusion gradient composite tool materials were prepared by five steps. Firstly, the starting TiB_2—TiC and Ti(C_7N_3) powders were separately ball-milled using WC balls and ethanol as the medium for 24 h, and then dried in a vacuum dry evaporator.

Table 1
Composition ratios of self-diffusion gradient cermet composite tool materials with different metal binder.

Symbols	TiB_2—TiC	Ti(C_7,N_3)	VC	Ni	Co	Mo	Remarks
S1	88		4	4		4	Surface layer
S2	86		4	6		4	Surface layer
S3	84		4	8		4	Surface layer
S4	82		4	10		4	Surface layer
M1		88		8	0	4	Substrate
M2		88		5.6	2.4	4	Substrate
M3		88		3.2	4.8	4	Substrate
M4		88		1.6	6.4	4	Substrate
M5		88		0	8	4	Substrate
M6		86		10		4	Substrate
M7		84		12		4	Substrate
M8		82		14		4	Substrate

Table 2
Sintering process parameters for self-diffusion gradient cermet composite tool materials.

Symbols	Sintering temperature (°C)	Holding time (min)	Heating rate (°C/min)	Hot pressure (MPa)
P1	1475	30	20	32
P2	1475	30	25	32
P3	1475	30	30	32
P4	1475	30	35	32

Table 3
Composition and sintering process of self-diffusion gradient composite tool materials.

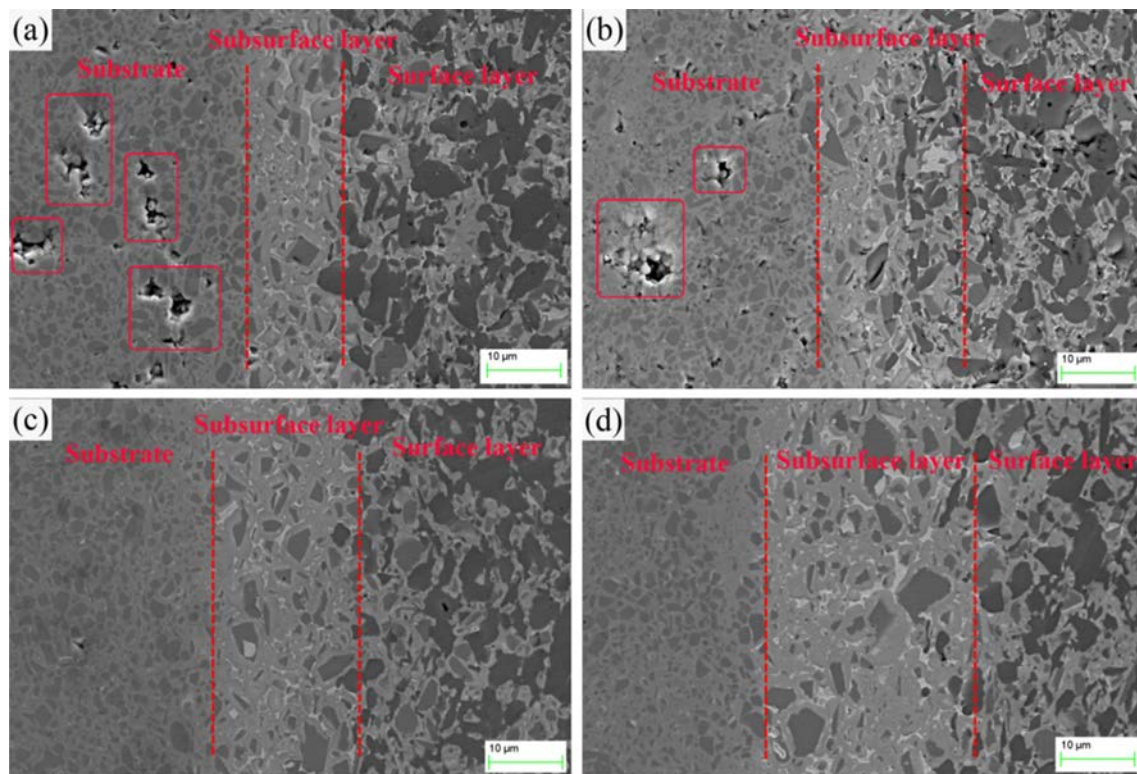| Symbols	Substrate composition	Surface layer composition	Sintering process	Ni/(Co + Ni) in substrate
M3-S4-P1	M3	S4	P1 (20 °C/min)	0.4
M3-S4-P2	M3	S4	P2 (25 °C/min)	0.4
M3-S4-P3	M3	S4	P3 (30 °C/min)	0.4
M3-S4-P4	M3	S4	P4 (35 °C/min)	0.4
M3-S1	M3	S1	P3	0.4
M3-S2	M3	S2	P3	0.4
M3-S3	M3	S3	P3	0.4
M1-S2	M1	S2	P3	1.0
M2-S2	M2	S2	P3	0.7
M4-S2	M4	S2	P3	0.2
M5-S2	M5	S2	P3	0.0
M6-S2	M6	S2	P3	1.0
M7-S2	M7	S2	P3	1.0
M8-S2	M8	S2	P3	1.0

Fig. 1. SEM micrographs of polished cross section for the samples sintered at different heating rates: (a) M3-S4-P1: 20 °C/min (b) M3-S4-P2: 25 °C/min (c) M3-S4-P3: 30 °C/min (d) M3-S4-P4: 35 °C/min.

Secondly, Mo, Ni and VC powders were added into the TiB_2–TiC powders as the surface layer, and the Mo, Ni and Co powders were added into the $Ti(C_7N_3)$ powder as the substrate. Then, these two mixed powders were separately ball-milled for 24 h and dried in a vacuum dry evaporator. Thirdly, the two mixed powders were sieved using a 200-mesh sieve. Fourthly, the substrate powder with 2.7 mm thickness and the surface layer powder with 400 μm thickness were put into a graphite die layer by layer, and then the green body was compressed under 10 MPa for 5 min. Finally, the green body was sintered by a hot-pressing process at 1475 °C and 32 MPa for 30 min with different heating rates of 20, 25, 30 and 35 °C/min (Table 2 shows the combinations of sintering parameters).
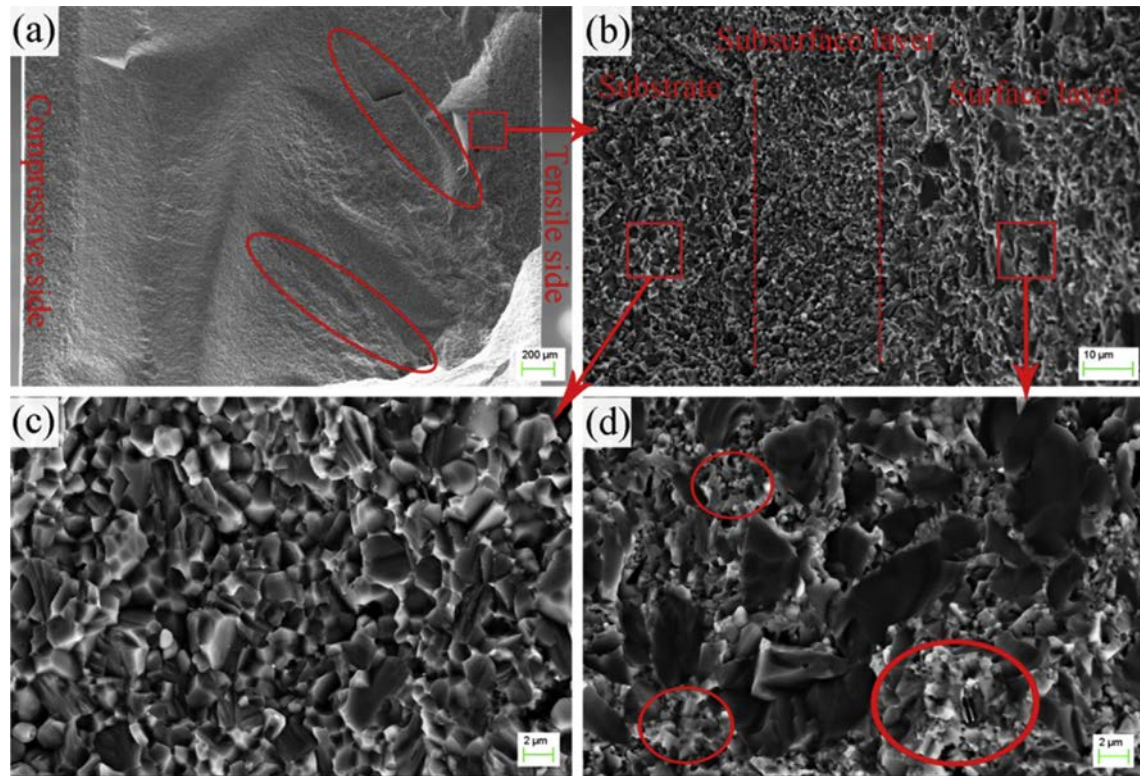
Fig. 2. SEM micrographs of fracture surfaces of the M3-S4-P4 sample sintered at a heating rate of 35 °C/min. (a) the whole fracture surface, (b) the gradient zone, (c) the enlarged substrate, and (d) the enlarged surface layer.
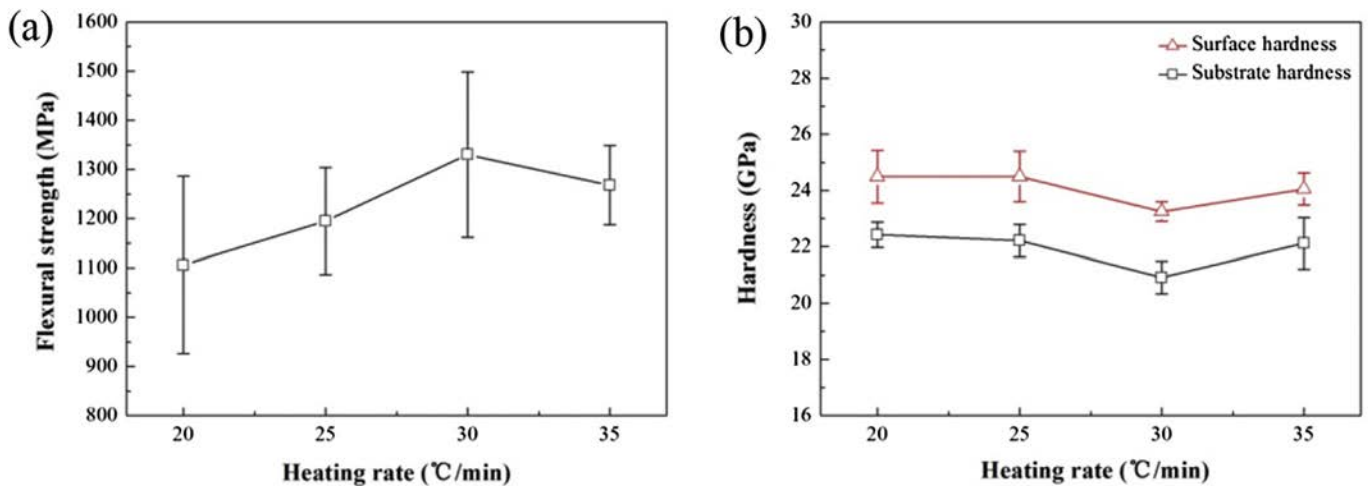

Fig. 3. Effects of heating rates on the (a) flexural strength and (b) hardness of the sintered samples (error bars show standard deviations).

Fourteen self-diffusion gradient composite tool materials with different combinations of the compositions and processes parameters are given in Table 3. The sintered disks were cut into blocks with the dimensions of 3 mm × 4 mm × 30 mm, and the surfaces and cross-sections were then ground and polished. Afterwards, the surface layer thickness was about 200–230 μm. The flexural strength was measured using a three-point bending tester (Model WDW-50E, Shidai, China) with a span of 20 mm and a loading velocity of 0.5 mm/min. The surface hardness and substrate hardness were measured using a Vickers hardness tester (HV$_1$, HVS-1000, Hugong, China) on the polished surface layers and cross-sections with a load of 9.8 N and a dwell time of 15 s, respectively. The phase composition for each sample was characterized by

an X-ray diffraction (XRD, Hitachi RAX-10A-X) with Cu Kα$_1$ radiation ($\lambda = 1.54050$ Å) and a scanning step of 4°/min. The microstructure of cross-sections and the fractured surfaces were observed using scanning electron microscopy (SEM, SUPRA55, Zeiss, Germany) equipped with energy-dispersive spectrometry (EDS, PV9900, Philips, Netherlands).

3. Results and discussion

3.1. Effects of heating rate

3.1.1. Microstructure

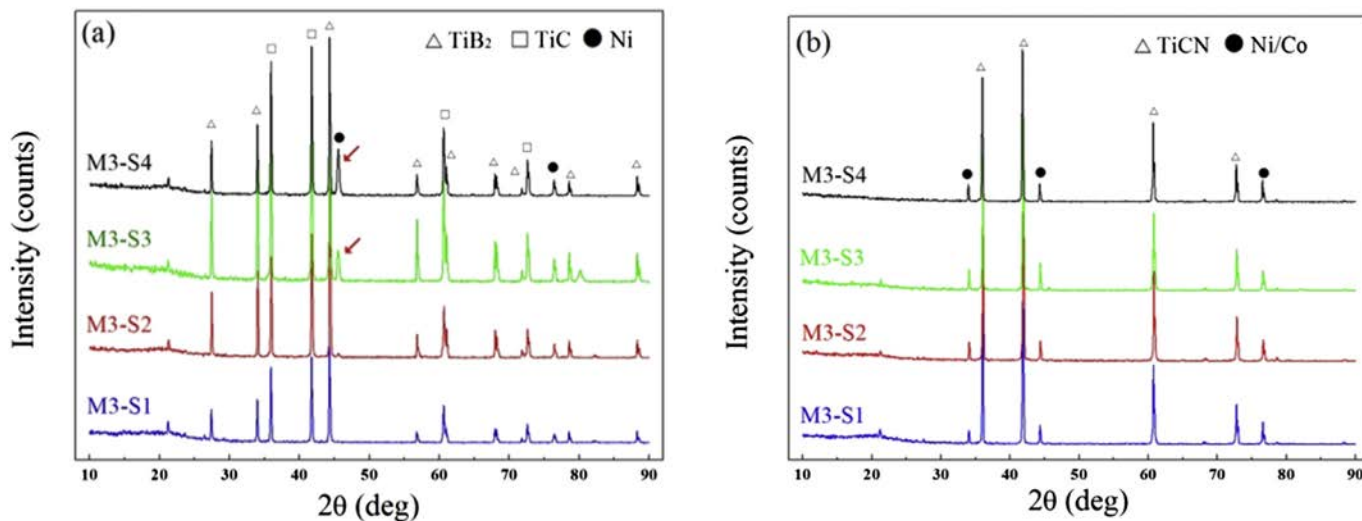Fig. 1 shows SEM micrographs of polished cross sections for the

Fig. 4. XRD patterns of (a) surface layer and (b) substrate of four samples with different Ni contents in the surface layer. M3-S1: 4 mass% Ni, M3-S2: 6 mass% Ni, M3-S3: 8 mass% Ni, M3-S4:10 mass% Ni.

samples sintered at different heating rates. During liquid phase sintering, a subsurface layer with 10–30 μm thickness was formed by self-diffusion driving force. This layer is characterized by an abundant white phase. According to our previous study [22], the white phase is metal binder such as Co and Ni. The metal binder in the substrate layer leads to an improvement of mechanical properties and an enhancement of interface strength between the substrate and surface layer. The binder-rich subsurface layer acts as a tough layer in the composite, which can strengthen the effect of grain pulling-out and absorb the crack propagation energy. The formation process of gradient composites can be divided into the following three stages. Firstly, Ti(C,N) is decomposed at high temperature in a vacuum denitrifying condition. After the appearance of the liquid phase, Ti(C,N) is expected to decompose as Ti, C and N and dissolve into the liquid binder. Secondly, the N element diffuses outward under vacuum, resulting in a decrease of N activity and the formation of vacancies or voids. The Ti element diffuses in the opposite direction due to the thermodynamic coupling effects between the N and Ti elements. Finally, the Ni and Co binder phases flow into the vacancies under the hot-pressure conditions. Hence, a subsurface layer with metal binder enrichment is formed.

The thickness of subsurface layer and, hence, the white phase in the subsurface layer increase with an increase in the heating rate, as shown in Fig. 1. This increase is attributed to the reduced loss of metal binder (the white phase) within the shorter heating time associated with a higher heating rate. The loss of metal binder can be proved by the solidified metal that was found on the inner walls of the graphite die. The loss of metal binder can be attributed to two aspects. Firstly, a small amount of metal binder will be evaporated at a high sintering temperature, which leads to the loss of metal binder. Secondly, during sintering at a high temperature the metal binder is in a liquid state and the liquid metal binder may flow out from the sintered body to the inner walls of the graphite die under a high sintering pressure.

Some pores are observed in the substrate of the samples sintered at the heating rates of 20 and 25 °C/min, as shown by rectangles in Fig. 1(a) and (b). By contrast, no pores are found in the substrate of samples sintered at the heating rates of 30 and 35 °C/min (Fig. 1(c) and (d)). It is believed that the formation of porosities is mainly attributed to the excessive decomposition of Ti(C,N), the extent to which increases with the heating time. The decomposition of Ti(C,N) leads to the formation of N_2 which will escapes from

the sintering body in a vacuum condition [26]. But excessive decomposition of Ti(C,N) occurs with a longer heating time resulting in the formation of pores. Meanwhile, there is no sufficient metal binder to fill in the pores due to the loss of metal binder. As a result, pores are left in the substrate of the samples sintered at a lower heating rate.

Fig. 2 shows the SEM micrographs of fracture surfaces of the M3-S4-P4 sample sintered at a heating rate 35 °C/min. The fracture surfaces are inspected to observe crack initiation sites, crack propagation evidence and fracture mode. Fracture failure can be characterized by three stages: crack initiation, crack propagation and final fracture. Cracks tend to initiate at grain boundaries, inclusions, pores and other microstructural defects. In Fig. 2(a), the cracks might be initiated from the tensile side under the three point bending load and propagated towards the compressive side. Although Ti(C,N) and TiB_2 are brittle materials, the plastic fracture stripes (shown in ellipses in Fig. 2(a)) can clearly be observed on the fracture surface. The plastic fracture mode for brittle material is attributed to the addition of Ni and Co metal binder. The surface layer, subsurface layer and the substrate of the fracture surface are found to have different characteristics as shown in Fig. 2(b)-(d). The main fracture mode of the surface layer is a mixture of transgranular and intergranular fracture. However, there are some fine grains (shown in circles in Fig. 2(d)), which lead to a positive effect on the flexural strength according to the Hall-Petch relationship. By contrast, the main fracture mode of the subsurface layer appears to be only intergranular fracture due to the aggregation of metal binder. Interestingly, the substrate shows a homogenous and compact microstructure with the grain size of about 1 μm, which is ideal for the substrate of the function-graded materials. Nevertheless, it may be stated that the fracture of the sintered samples is characterized by brittle crack in spite of some plastic stripes.

3.1.2. Mechanical properties

Fig. 3 shows the effects of heating rates on the flexural strength and hardness of the samples sintered at four different heating rates. It can be noticed that the flexure strength increases initially when the heating rate is increased from 20 to 30 °C/min, but it decreases as the heating rate is further increased to 35 °C/min with a maximum turning point at 30 °C/min. A reverse trend is found for the surface hardness and substrate hardness with respect to the heating rate where the minimum turning point is found at the
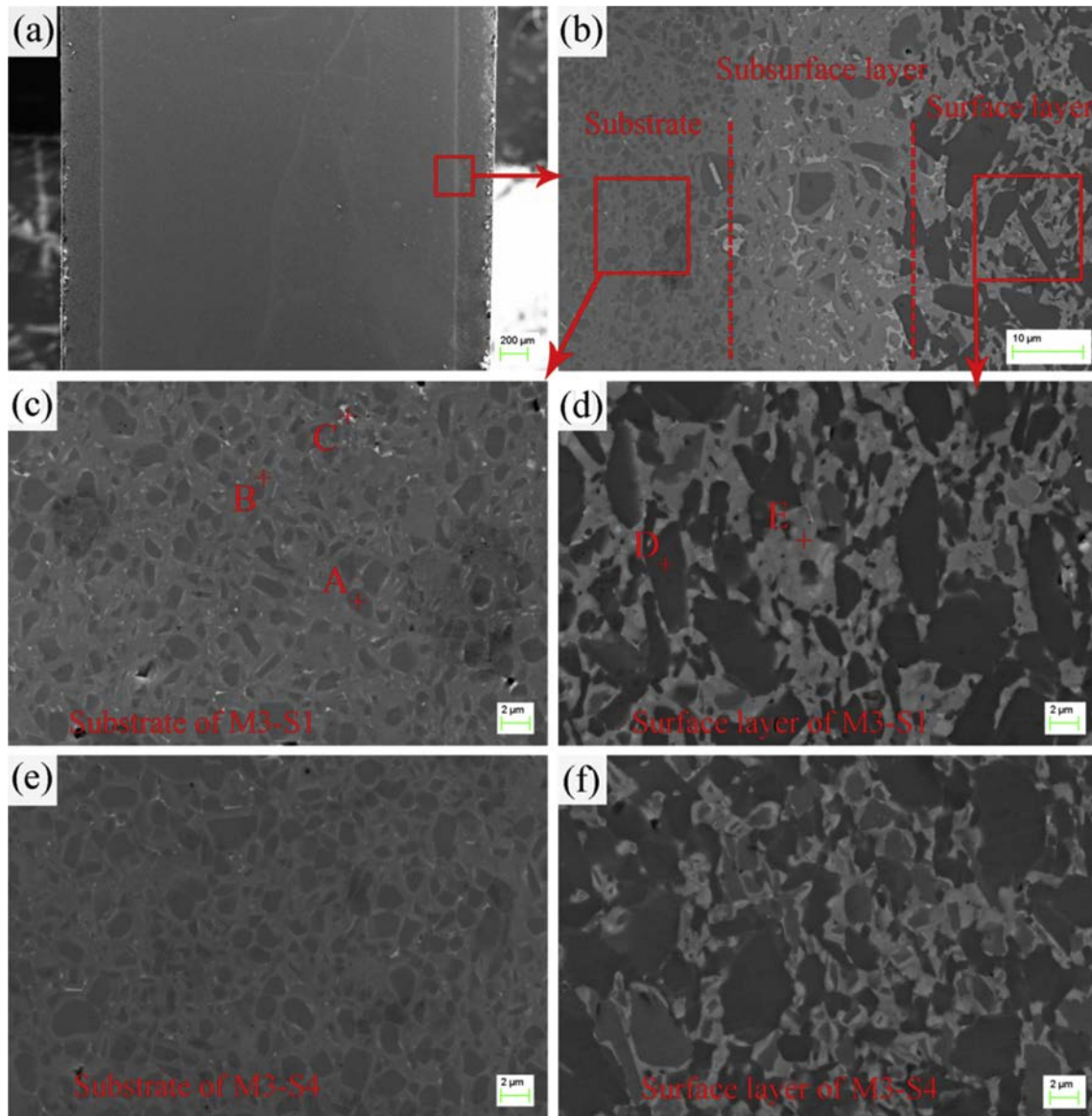
Fig. 5. SEM micrographs of polished surface of self-diffusion gradient composites with different Ni contents in the surface layer. (a) the sample overview, (b) a cross section of M3-S1, (c) the substrate of M3-S1, (d) the surface layer of M3-S1, (e) the substrate of M3-S4, and (f) the surface layer of M3-S4.

heating rate of 30 °C/min. Quantitatively, the experimental results reveal that the heating rate has a greater effect on the flexural strength than the hardness; the former has a about 20% variation while the latter has about 5% when the heating rate is changed from 20 to 35 °C/min. It is noted that the increase of flexural strength when the heating rate is increased from 20 to 30 °C/min is attributed to the increase of material density and subsurface layer thickness. It should be noted that the sample sintered at the heating rate of 35 °C/min exhibits the maximum thickness of subsurface layer, but a decrease in flexural strength as compared to those at the 30 °C/min heating rate. The subsurface layer with metal binder enrichment has a high toughness but a low strength, so an excessive thickness of subsurface layer is adverse to the improvement of the flexural strength. The thickness of subsurface layer is about 30 μm for the sample sintered at the heating rate of 35 °C/min, while that is about 20 μm for the sample sintered at the heating rate of 30 °C/min. Therefore, 20 μm is a favorable thickness of subsurface layer for self-diffusion gradient composites.

The above analysis indicates that for the investigated range of heating rates, the samples sintered at the heating rate of 30 °C/min shows the highest flexural strength (at 1330 ± 168 MPa for the M3-S4-P3 sample), while the hardness is also good with only a marginal decrease. For the M3-S4-P3 sample, the substrate hardness is 20.92 ± 0.38 GPa and surface hardness is 23.25 ± 0.34 GPa. Thus, 30 °C/min is in the vicinity of the optimum heating rate for the sintering process of the composite materials under investigation.

3.2. Effects of metal binder

3.2.1. Effects of Ni content in the surface layer

Fig. 4 shows the XRD patterns of surface layer and substrate of four samples with different Ni content in the surface layer. In the surface layer, two main phases are found to be TiB_2 and TiC, while in the substrate the main phase is Ti(C,N) which indicates that strong reactions did not happen during liquid phase sintering. Mo and VC are not found in the XRD patterns due to their lower content. Two
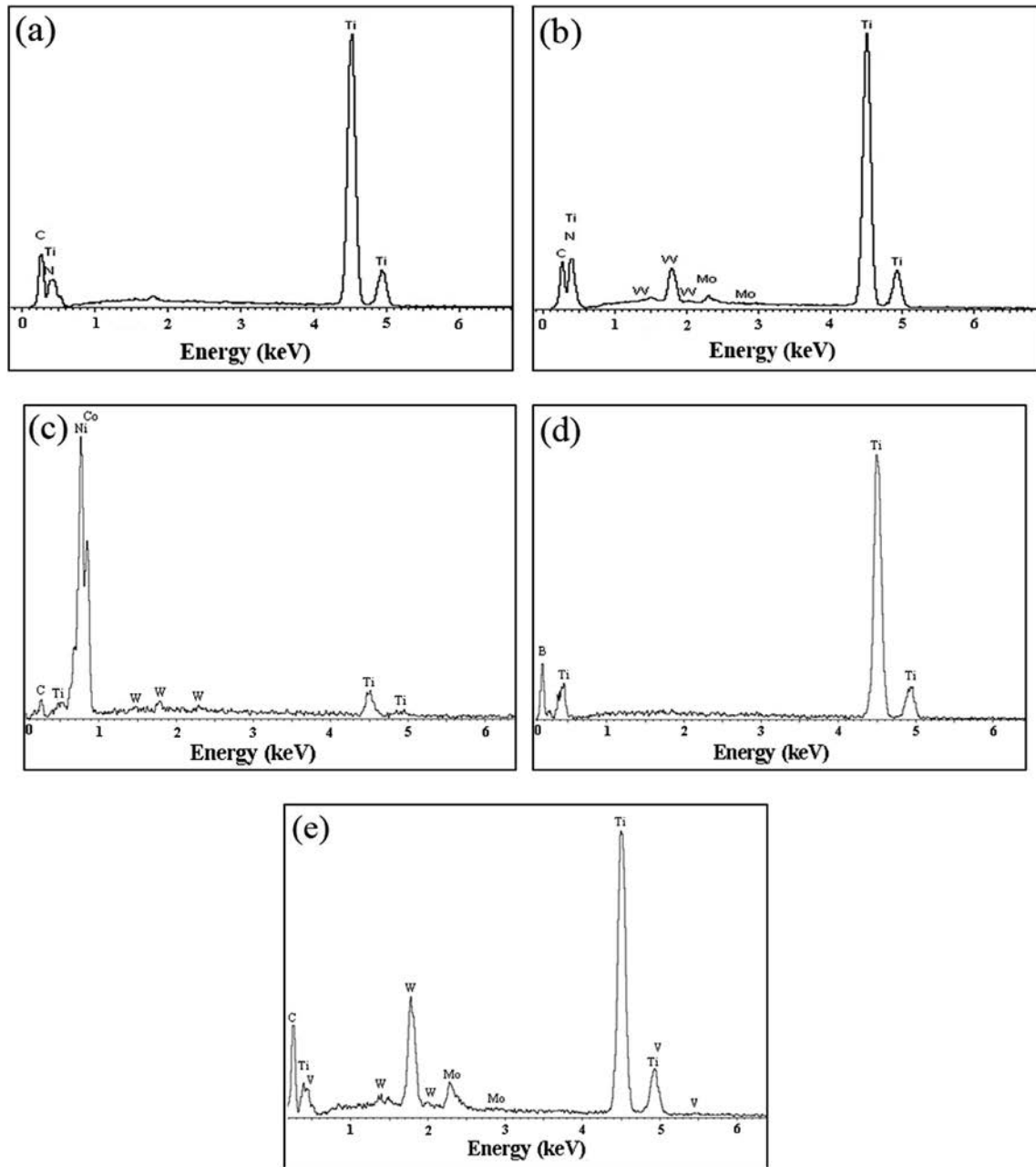
Fig. 6. EDS images for the surface layer and substrate of self-diffusion gradient composites. (a), (b) and (c) correspond to Points A, B and C in Fig. 5(c), respectively, and (d) and (e) correspond to points D and E in Fig. 5 (d), respectively.

peaks at about 45° (shown by the arrows in Fig. 4(a)) corresponding to Ni binder are found in the surface layer of the M3-S3 and M3-S4 sample, but are not found for the M3-S1 and M3-S2 sample. With increasing Ni binder content, the relative intensity of this peak at 45° increases indicating that the Ni content in the surface layer increased, as shown in Fig. 4(a).

Fig. 5 displays the SEM micrographs of polished surfaces of self-diffusion gradient composites with different Ni contents in the surface layer. The substrate of the samples as shown in Fig. 5(c) and (e) is comprised of black core phase, gray rim phase and white phase, while the surface layer is comprised of black phase and gray phase, as shown in Fig. 5(d) and (f). To ascertain these different phases in the composite, multiple representative points were selected, as shown by Points A-E in Fig. 5(c) and (d), to perform EDS

analysis. Fig. 6(a)-(c) indicate that the black phase (as in Point A in Fig. 5(c)), the gray phase (as in Point B in Fig. 5(c)) and the white phase (as in Point C in Fig. 5(c)) are the Ti(C,N) phases, (Ti,W,-Mo)(C,N) solid solution and Ni binder in the substrate, respectively. Fig. 6(d) reveals that black phase in the surface layer (as in Point D in Fig. 5(d)) contains the titanium and boron, indicating that it is TiB_2 phase. Fig. 6(e) reveals that the gray phase in the surface layer (as in Point E in Fig. 5(d)) contains the titanium, carbon, vanadium, molybdenum and tungsten elements, confirming the presence of (Ti,W,Mo,V)C solid solution phase. The tungsten in the composites may be derived from the abrasion of WC balls during the ball milling of the starting powders. A full densification is achieved for all samples and no remarkable porosities or cracks were found on the polished surfaces. This is consistent to the earlier analysis on
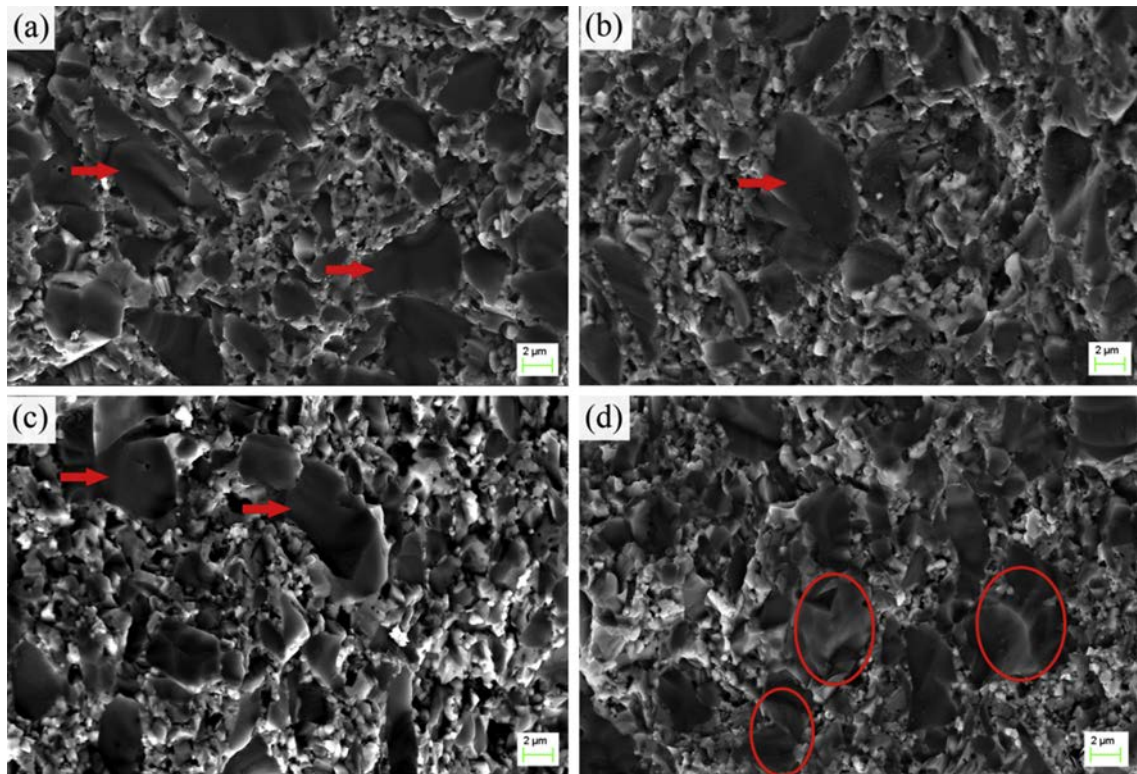
Fig. 7. SEM micrographs of fractured surface layer of self-diffusion gradient composites with different Ni contents in the surface layer. (a) M3-S1: 4 mass% Ni (b) M3-S2: 6 mass% Ni (c) M3-S3: 8 mass% Ni (d) M3-S4: 10 mass% Ni.
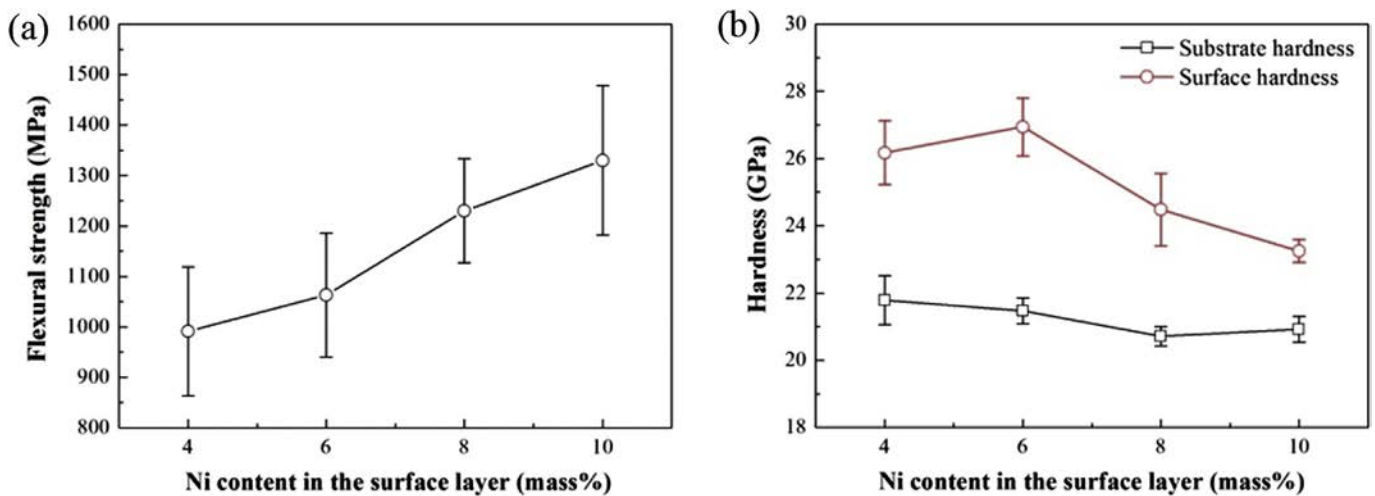

Fig. 8. Effects of Ni content in the surface layer on (a) the flexural strength and (b) the hardness of fabricated self-diffusion gradient composites (error bars show standard deviations). M3-S1: 4 mass% Ni, M3-S2: 6 mass% Ni, M3-S3: 8 mass% Ni, and M3-S4: 10 mass% Ni.

the effect of heating rate. A black core-gray rim structure in Ti(C,N)-based cermet is formed by Ostwald's dissolution-precipitation theory [27,28]. This supports the finding in this study. According to the thermodynamics, smaller particles are dissolved more easily than larger particles. During liquid phase sintering at the temperature above 1300 °C, W and Mo can dissolve into the liquid binder phases. When a saturation status is reached, W and Mo will reprecipitates from liquid phase to black core phases of the undissolved Ti(C,N) particles, forming gray rim phases of the (Ti,W,Mo)(C,N) solid solution. As a result, a black core−gray rim structure is formed. Fig. 7 shows the SEM micrographs of some

fractured surface layers of the sintered composites with different Ni contents in the surface layer. It is found that coarse TiB_2 grains exhibit transgranular fracture (as shown by arrows in Fig. 7). Uneven characteristics can be found in the fractured surface of TiB_2 grains (as shown in circles in Fig. 7(d)).

Fig. 8 shows the variation of flexural strength and hardness of the fabricated composites with respect to the Ni content in the surface layer. It shows that with an increase in the Ni content in the surface layer, the flexural strength increases monotonically with its maximum of 1330 MPa at 10 mass% Ni binder content. Attempts to further increase the Ni content are not made in this study. By
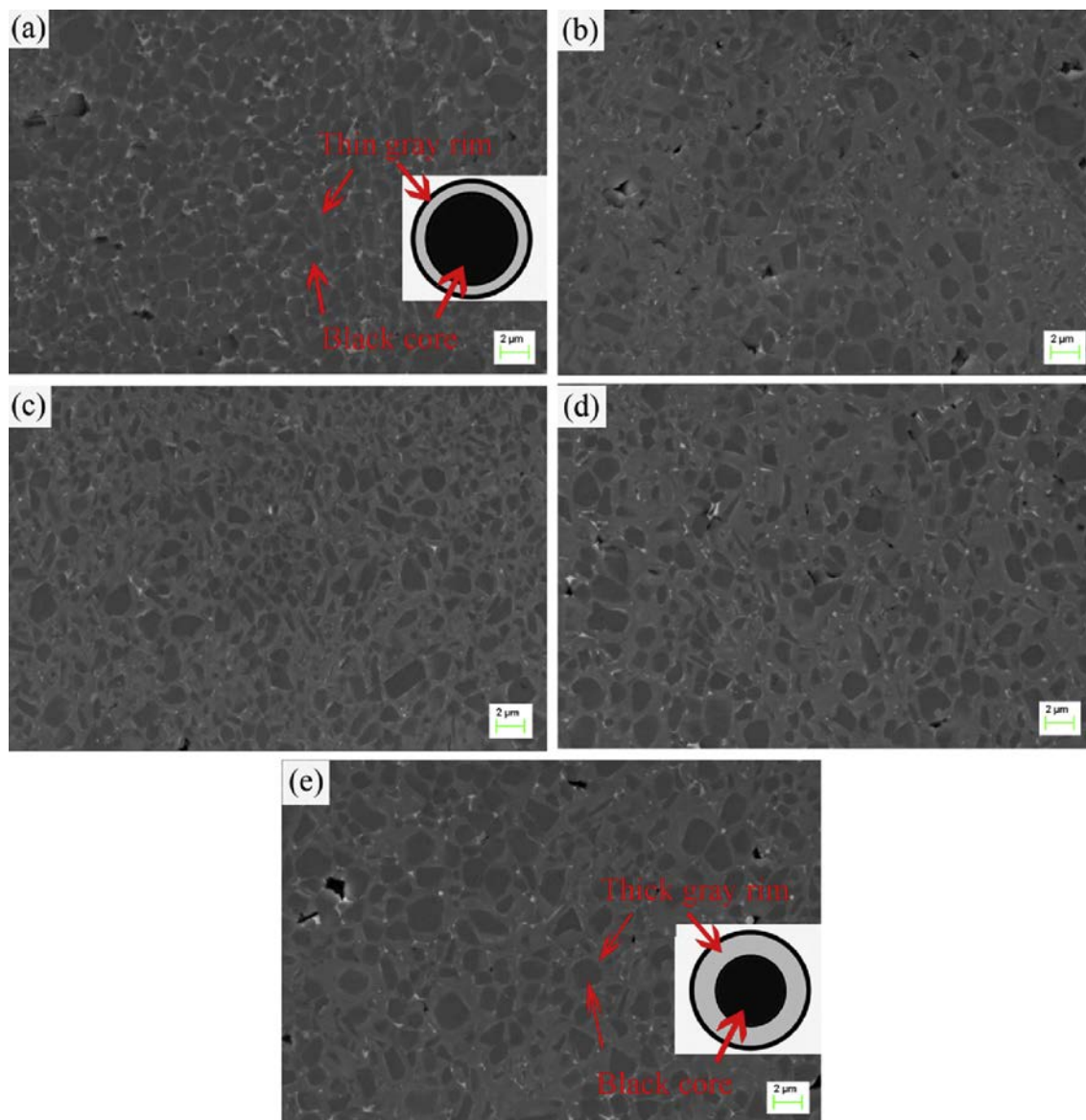
Fig. 9. SEM micrographs of polished substrates of self-diffusion gradient composites with different Ni/(Co + Ni) mass ratios in the substrate. (a) M1-S2: 1.0, (b) M2-S2: 0.7 (c) M3-S2: 0.4, (d) M4-S2: 0.2, (e) M5-S2: 0.0.

contrast, the surface hardness increases initially with the Ni content, but then decreases, while the substrate hardness changes very slightly with a very marginal decrease, as shown in Fig. 8. As shown in Fig. 5(d) and (f), a higher Ni content in the surface layer yields more homogeneous and uniform grains than a lower Ni content which, according to [12], should result in a higher density and higher flexural strength. Likewise, a higher density caused by a higher Ni content is associated with an increase in the surface hardness. However, as the Ni content is further increased, the excessive Ni binder leads to a reduced surface hardness since Ni has a lower hardness than the hard particles in the surface layer. As a result, the relationship between the surface hardness and Ni content has a peak point at 6 mass% of Ni content. During the liquid sintering process, it is possible that a small amount of Ni is transferred to the substrate to cause a decrease its hardness. However, this decrease is small as shown in Fig. 8(b). When considering all the three mechanical properties jointly, a Ni content of 6−8 mass% may be used for the surface layer. If a 6 mass% Ni is used, the

flexural strength, substrate hardness and surface hardness for the M3-S2 sample are 1063 ± 123 MPa, 21.47 ± 0.39 GPa and 26.94 ± 0.86 GPa, respectively.

3.2.2. Effects of Ni/(Co + Ni) ratio in the substrate

Fig. 9 shows the SEM micrographs of polished substrates of the composites with different Ni/(Co + Ni) ratios in the substrate. It can be seen that samples can be sintered to a high density irrespective of the metal binder composition from pure Ni over Ni−Co alloys to pure Co binder. It is found that a typical black core-gray rim structure is embedded into the white metal binder network. It is believed that the black cores are undissolved Ti(C,N) particles, while the gray rims are (Ti,W,Mo)(C,N) solid solution. Further, the composites with pure Ni binder exhibits a thinner rim phase than that with the Co binder. This may be due to the fact that the W and Mo elements are more soluble in the Co binder than in the Ni binder, mainly because the atomic radius of Co is much similar with W and Mo than that of Ni. A complete surrounding phase will
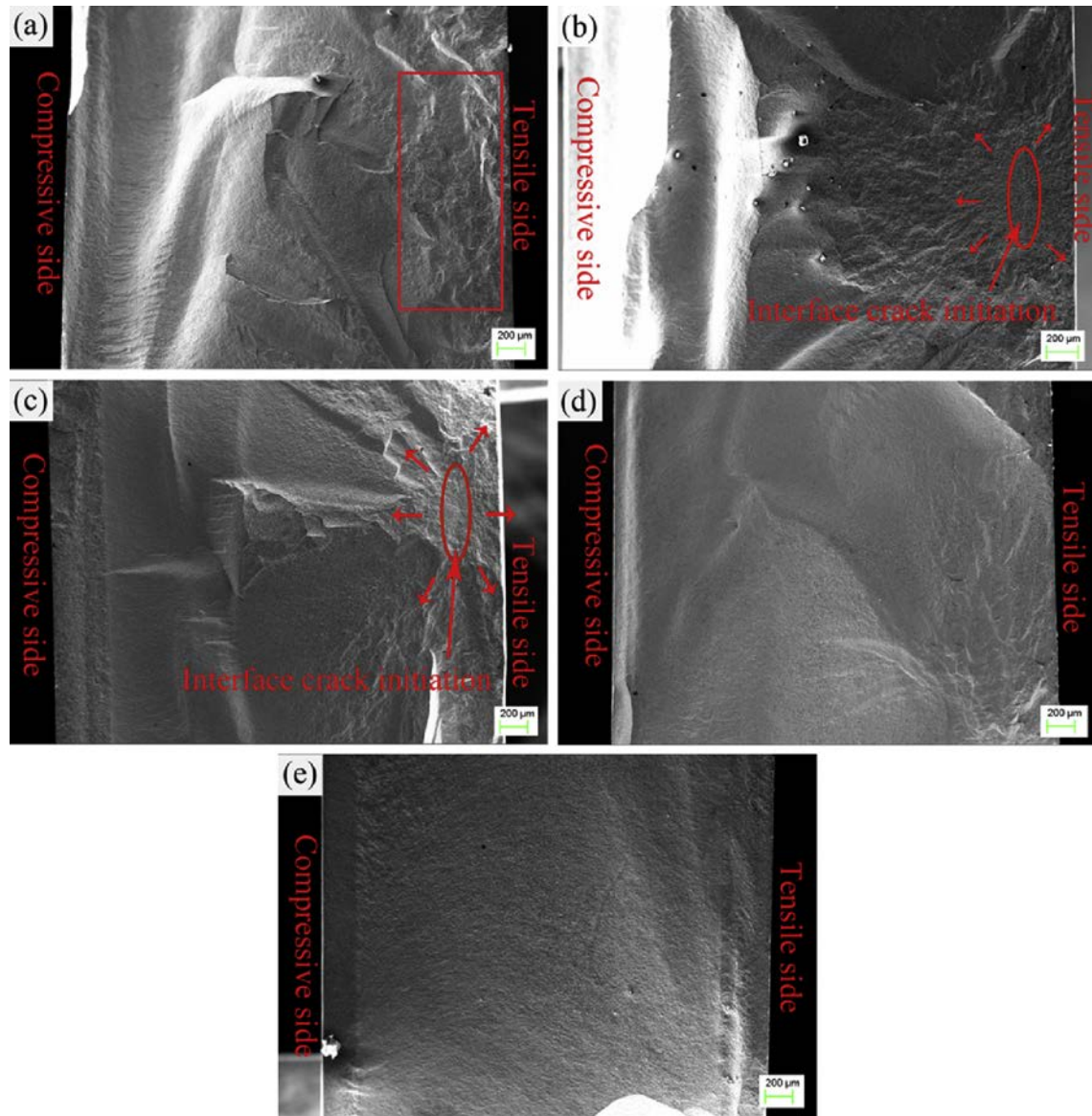
Fig. 10. SEM micrographs of fractured surfaces of self-diffusion gradient composites with different Ni/(Co + Ni) ratios in the substrate. (a) M1-S2: 1.0, (b) M2-S2: 0.7 (c) M3-S2: 0.4, (d) M4-S2: 0.2, (e) M5-S2: 0.0.

increase the bonding strength between the hard phase and binder phase and suppress the crack propagation in the cermets. As a result, the flexural strength of the cermets is improved. However, it has been reported that the flexural strength sharply decreases at the rim thickness of 0.5 μm or larger as the rim phase is brittle in nature [4].

Fig. 10 shows the SEM micrographs of fractured surfaces of self-diffusion gradient composites with different Ni/(Co + Ni) ratios in the substrate. The fractured surface becomes more flat when the Co content is increased. The fractured surface with pure Ni binder exhibits a plastic deformation (as shown in the rectangle Fig. 10(a)), but it is not found in the sample with pure Co binder (Fig. 10(e)). The interface crack initiation is found in Fig. 10(b) and (c), but cracks originate from the surface layer of tensile side in Fig. 10(a), (d) and (e). The formation of interface crack is attributed to the stress concentration in the interface resulting from the mismatch of coefficients of thermal expansion (CTE) between surface layer and substrate. Due to the mismatch of CTE, residual stresses develop in

the laminated composites during the cooling process [29]. The magnitude of the residual stresses is proportional to the CTE mismatch and has a crucial effect on the mechanical properties of the composites. It has been reported that the surface compressive residual stress is beneficial to flexural strength of laminated composites [30,31]. In the self-diffusion gradient cermet composite fabricated in this study, compressive residual stresses are formed in the surface layer due to its smaller CTE. But, a large stress concentration at the interface between the surface layer and the substrate will be generated due to the action of the residual thermal stresses. As a result, the cracks are prone to initiate and extend at the interface resulting in a decrease in flexural strength. The CTE of Ni is larger than that of Co, which is beneficial to reduce the CTE mismatch between surface layer and substrate. Further, as discussed earlier the addition of Ni binder can actually improve the grain boundary strength due to the thinner rim phase. Therefore, the pure Ni is a better metal binder than pure Co and the mixture of Co and Ni.
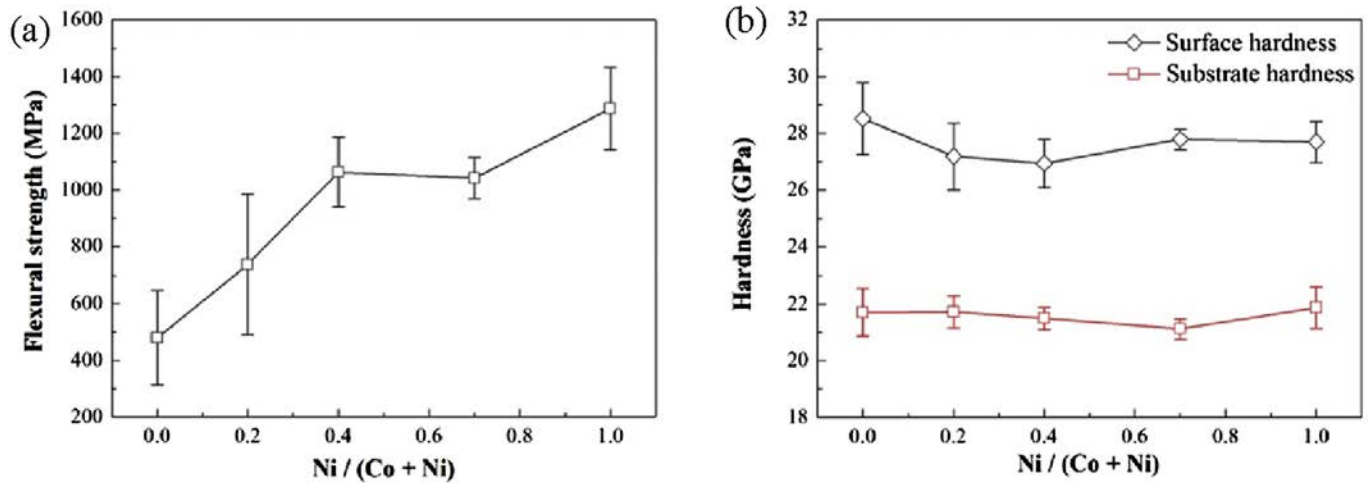
Fig. 11. Effects of Ni/(Co + Ni) ratio on the (a) flexural strength and (b) hardness of self-diffusion gradient composites. M1-S2: 1.0, M2-S2: 0.7, M3-S2: 0.4, M4-S2: 0.2, and M5-S2: 0.0.
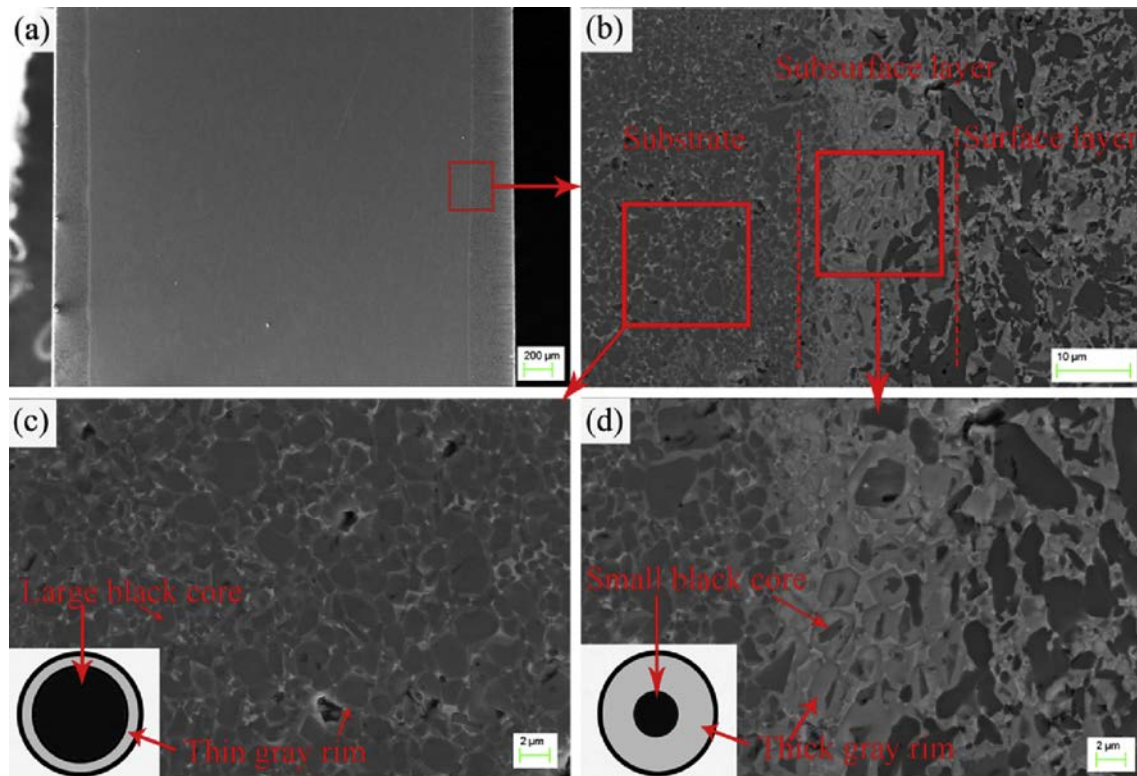

Fig. 12. SEM micrographs of polished surface of the sample M8-S2 with 14 mass% Ni binder in the substrate showing that excessive Ni binder leads to coarse grains in subsurface layer with a thick gray rim and small black core. (a) the sample overview (b) an enlarged cross section (c) the enlarged substrate (d) the enlarged subsurface layer.

Fig. 11 shows the effects of the Ni/(Co + Ni) ratio in the substrate on the mechanical properties of the fabricated composites. It can be seen that with increasing Ni/(Co + Ni) ratio in the substrate the flexural strength increases remarkably, while the surface hardness and substrate hardness both exhibits minor variations. The flexural strength, substrate hardness and surface hardness of the sample using pure Ni binder are 1287 ± 146 MPa, 21.87 ± 0.73 GPa and 27.70 ± 0.73 GPa, respectively, while those for pure Co binder are 480 ± 167 MPa, 21.71 ± 0.85 GPa and 28.52 ± 1.07 GPa, respectively. The differences are attributed to the following facts. Since Co is harder than Ni, samples with Co binder are expected to be harder

than those with the Ni binder. However, the harder Co binder results in the composites to have a lower flexural strength. Further, the Ni binder can result in thinner rim phases and a smaller CTE mismatch between the surface layer and the substrate, which both are beneficial to the improvement of the flexural strength. Therefore, the Ni binder is favoured for the self-diffusion gradient composites.

3.2.3. Effects of Ni content in the substrate

Fig. 12 displays some SEM micrographs of polished surface of the M8-S2 self-diffusion gradient composite with 14 mass% Ni in the
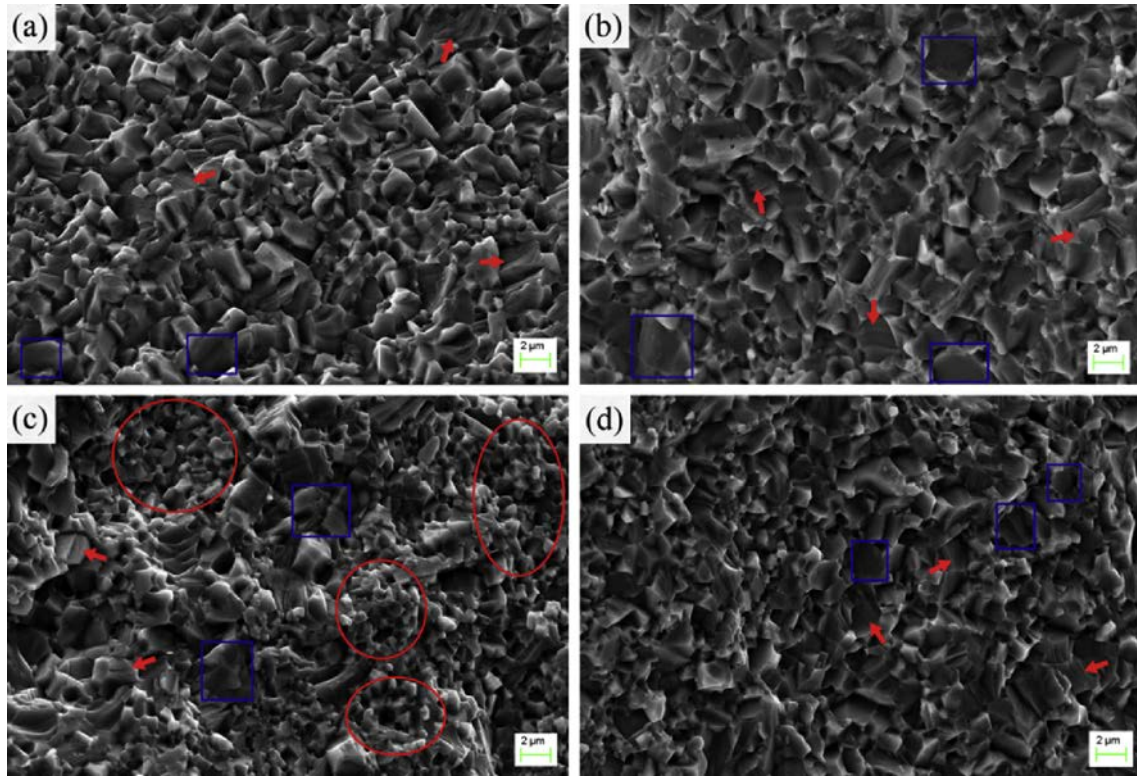
Fig. 13. SEM micrographs of substrate fractured surfaces of self-diffusion gradient composites with different Ni binder contents in the substrate: (a) M1-S2: 8 mass% Ni, (b) M6-S2: 10 mass% Ni, (c) M7-S2: 12 mass% Ni, and (d) M8-S2: 14 mass% Ni.
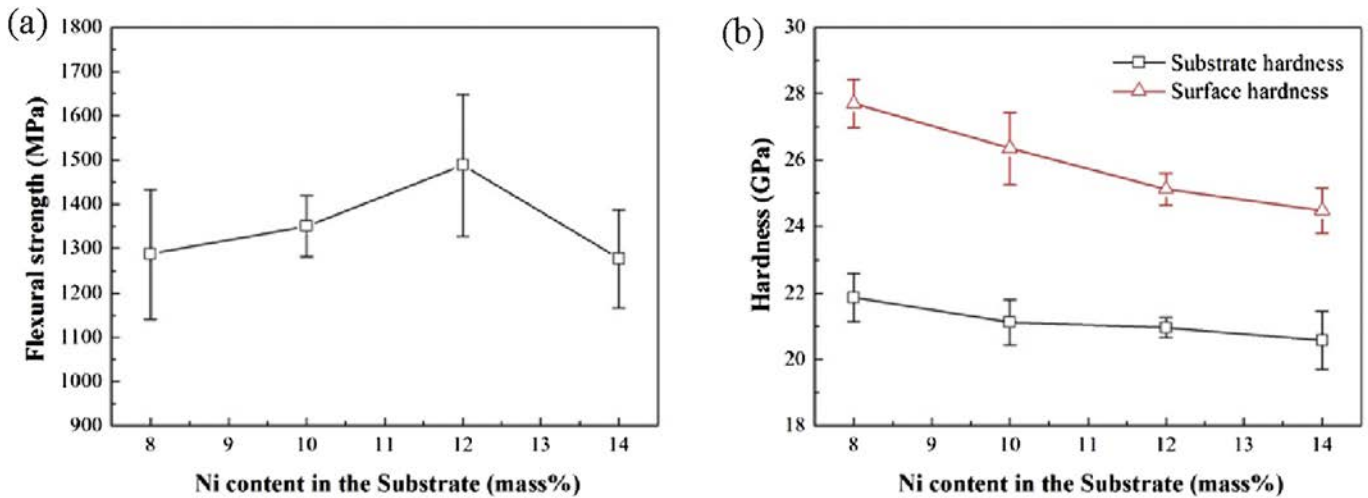

Fig. 14. Effects of Ni content in the substrate on the (a) flexural strength and (b) hardness of the self-diffusion gradient composites (error bars show standard deviations). M1-S2: 8 mass% Ni, M6-S2: 10 mass% Ni, M7-S2: 12 mass% Ni, and M8-S2: 14 mass% Ni.

substrate. The dense samples with about 200 μm thickness surface layer are obtained by the addition of Ni binder. It is observed that the phase composition and grain morphology of the substrate do not change with increasing Ni binder content (Figs. 9(a) and 12(c)). The globular grains of Ti(C,N) are uniformly dispersed in Ni binder network. The hard Ti(C,N) particles surrounded by thin rim phases make a perfect black core-gray rim structure with a thin rim, which improves the mechanical properties. However, the grains in the subsurface layer becomes coarser with increasing Ni binder content. Furthermore, the morphology of grains changes into a small

black core-thick gray rim structure (Fig. 12(d)), which is detrimental to the mechanical properties. The formation of this small core-thick rim structure is attributed to the strong solid solution reaction induced by the excessive Ni liquid phase in the sintering process. With increasing Ni content in the substrate, the Ni content in the subsurface layer also increases and more volume of the Ti(C,N) particles are dissolved in the Ni liquid phase. The black cores, which are undissolved part of Ti(C,N) particles, become smaller. When saturation concentration status of the Ni liquid phase is reached, the (Ti,W,Mo)(C,N) solid solution precipitates on

the black core resulting in the thick gray rims. Therefore, the small black core-thick gray rim structure is formed, shown as in Fig. 12(d).

Fig. 13 shows the SEM micrographs of fractured surface at the substrate of self-diffusion gradient composites with different Ni binder contents in the substrate. Unlike in the surface layer, the main fracture mode of the substrates is found to be intergranular fracture and transgranular fracture. Cleavage pattern (shown in arrows in Fig. 13) and small facets (shown in rectangles in Fig. 13) are also observed on the large grains of the fractured surfaces, while the fine grains present intergranular fracture characteristics (shown in circles in Fig. 13). Overall, brittle rupture appears to be the main fracture characteristics on the fractured surfaces of the substrates.

The effects of Ni binder content in the substrate on the flexural strength and hardness of fabricated composites is shown in Fig. 14. It can be seen that an increase in the Ni binder content in the substrate until 12 wt% results in a monotonic increase in the flexural strength. However, further increasing the Ni content causes a decrease in the flexural strength. By contrast, the surface hardness and substrate hardness all decreases monotonically with an increase in the Ni binder content. The flexural strength, substrate hardness and surface hardness of M7-S2 containing 12 mass% Ni binder in the substrate are found to be 1488 ± 190 MPa, 20.96 ± 0.30 GPa and 25.12 ± 0.48 GPa, respectively. In general, increasing Ni binder content results in an increase in the density of the composites and hence an increase in the flexural strength. However, the Ni binder has a lower hardness than the hard particles and as its content is increased, the hardness of the composites decreases [12]. It is noted that the improvement of flexural strength is mainly attributed to the binder phases and the increase of density. But, at high Ni content such as 14 mass% Ni content in the substrate, it has been found as shown in Fig. 12(d) that the small black core-thick gray rim structure in the subsurface layer is formed, which decreases the flexural strength. Furthermore, a higher Ni binder content will result in a thicker binder between ceramic particles which leads to a decrease in the grain boundary strength. For the above reasons, the flexural strength shows a decreasing trend when the Ni content in the substrate is greater than 12 mass%.

4. Conclusions

Self-diffusion gradient composite tool materials were fabricated with different metal binder content and Ni/(Co + Ni) ratios under different heating rates in the sintering process. It has been found that:

(1) The heating rate has a significant effect on the flexural strength of the composites, but the effect is relatively small on the hardness. The improvement of the flexural strength is attributed to a high density and 20 μm thickness of subsurface layer. The sample sintered at the heating rate of 30 °C/min exhibits the highest flexural strength. For the M7-S2 sample, the flexural strength is 1488 ± 190 MPa, while its substrate hardness is 20.96 ± 0.30 GPa and surface hardness is 25.12 ± 0.48 GPa.

(2) With an increase in the Ni content in the surface layer, the flexural strength increases monotonically, but the surface hardness increases initially and then decreases, while the substrate hardness changes very slightly with a very marginal decrease. The improvement of flexural strength is attributed to the high density and fine microstructure.

(3) The composites with pure Ni exhibits a thinner rim phase than that with pure Co and the mixture of Co and Ni. W and Mo are more soluble in Co binder than Ni binder. Ni binder is

found to be more favorable than Co for enhancing the mechanical properties of the composites.

(4) Ni content in the substrate has a remarkable influence on the flexural strength and surface hardness. With an increase in the Ni binder content in the substrate, the flexural strength first increases and then decreases with a maximum turning point. The strength degradation is attributed to the formation of a small black core-thick gray rim structure and the decrease of grain boundary strength.

References

[1] S. Zhang, G.Q. Lu, Effect of the green state on the sintering of Ti(C,N)-based cermets, J. Mater. Process. Technol. 54 (1995) 29–33.
[2] K. Narasimhan, S.P. Boppana, D.G. Bhat, Development of a graded TiCN coating for cemented carbide cutting tools—a design approach, Wear 188 (1995) 123–129.
[3] P. Ettmayer, H. Kolaska, W. Lengauer, K. Dreyer, Ti(C,N) cermets—metallurgy and properties, Int. J. Refract. Met. Hard Mater. 13 (1995) 343–351.
[4] Y. Peng, H. Miao, Z. Peng, Development of TiCN-based cermets: mechanical properties and wear mechanism, Int. J. Refract. Met. Hard Mater 39 (2013) 78–89.
[5] Y. Liu, Y. Jin, H. Yu, J. Ye, Ultrafine (Ti, M)(C, N)-based cermets with optimal mechanical properties, Int. J. Refract. Met. Hard Mater 29 (2011) 104–107.
[6] B. Zou, C. Huang, J. Song, Z. Liu, L. Liu, Y. Zhao, Effects of sintering processes on mechanical properties and microstructure of TiB2–TiC+8wt% nano-Ni composite ceramic cutting tool material, Mater. Sci. Eng. A 540 (2012) 235–244.
[7] D. Wang, H. Wang, S. Sun, X. Zhu, G. Tu, Fabrication and characterization of TiB₂/TiC composites, Int. J. Refract. Met. Hard Mater. 45 (2014) 95–101.
[8] B. Zou, W. Ji, C. Huang, J. Wang, S. Li, K. Xu, Effects of superfine refractory carbide additives on microstructure and mechanical properties of TiB₂–TiC+Al₂O₃ composite ceramic cutting tool materials, J. Alloy Compd. 585 (2014) 192–202.
[9] D. Bucevac, V. Krstic, Microstructure–mechanical properties relations in SiC–TiB₂ composite, Mater. Chem. Phys. 133 (2012) 197–204.
[10] D. Vallauri, I.C. Atías Adrián, A. Chrysanthou, TiC–TiB₂ composites: a review of phase relationships, processing and properties, J. Eur. Ceram. Soc. 28 (2008) 1697–1713.
[11] S. Boudebane, S. Lemboub, S. Graini, A. Boudebane, A. Khettache, J. Le Lannic, Effect of binder content on relative density, microstructure and properties of complex cemented carbides obtained by thermal explosion-pressing, J. Alloy Compd. 487 (2009) 235–242.
[12] M. Gu, C. Huang, B. Zou, B. Liu, Effect of (Ni, Mo) and TiN on the microstructure and mechanical properties of TiB₂ ceramic tool materials, Mater. Sci. Eng. A 433 (2006) 39–44.
[13] X. Zhao, D. Zuo, M. Zhang, F. Xu, S. Feng, In situ production of ultra-fine Ti(C,N)–TiB₂–Co cermets by reactive hot processing from the Co–Ti–C–BN system, Int. J. Refract. Met. Hard Mater. 55 (2016) 1–10.
[14] M. Gu, H. Xu, J. Zhang, Z. Wei, A. Xu, Influence of hot pressing sintering temperature and time on microstructure and mechanical properties of TiB2/TiN tool material, Mater. Sci. Eng. A 545 (2012) 1–5.
[15] T.J. Davies, A.A. Ogwu, Characterisation of composite of TiC+TiB₂ bonded with nickel based binder alloy: mechanical and microstructural properties, Powder Metall. 38 (1995) 39–44.
[16] E. Conforto, D. Mari, T. Cutard, The role of molybdenum in the hard-phase grains of (Ti, Mo)(C, N)-Co cermets, Philos. Mag. 84 (2004) 1717–1733.
[17] X. Zhang, N. Liu, C. Rong, Effect of molybdenum content on the microstructure and mechanical properties of ultra-fine Ti(C,N) based cermets, Mater. Charact. 59 (2008) 1690–1696.
[18] A. Rajabi, M.J. Ghazali, A.R. Daud, Chemical composition, microstructure and sintering temperature modifications on mechanical properties of TiC-based cermet − a review, Mater. Des. 67 (2015) 95–106.
[19] W. Wang, Z. Fu, H. Wang, R. Yuan, Influence of hot pressing sintering temperature and time on microstructure and mechanical properties of TiB₂ ceramics, J. Eur. Ceram. Soc. 22 (2002) 1045–1049.
[20] L. Wang, H. Liu, C. Huang, B. Zou, X. Liu, Effects of sintering processes on mechanical properties and microstructure of Ti(C,N)–TiB₂–Ni composite ceramic cutting tool material, Ceram. Int. 40 (2014) 16513–16519.
[21] M. Shaw, Metal Cutting Principle, second ed., Oxford University, New York, 2005.
[22] B. Zou, W. Ji, C. Huang, S. Li, J. Wang, Study on microstructure and its

formation mechanism, and mechanical properties of TiB$_2$—TiC laminated Ti(C$_5$N$_5$) composite ceramic cutting tool material, Int. J. Refract. Met. Hard Mater. 42 (2014) 169—179.

[23] H. Zhou, C. Huang, B. Zou, H. Liu, H. Zhu, P. Yao, J. Wang, Effects of metal phases and carbides on the microstructure and mechanical properties of Ti(C,N)-based cermets cutting tool materials, Mater. Sci. Eng. A 618 (2014) 462—470.

[24] B. Zou, H. Zhou, K. Xu, C. Huang, J. Wang, S. Li, Study of a hot-pressed sintering preparation of Ti(C$_7$N$_3$)-based composite cermets materials and their performance as cutting tools, J. Alloy Compd. 611 (2014) 363—371.

[25] H. Zhou, C. Huang, B. Zou, H. Liu, H. Zhu, P. Yao, J. Wang, Effects of sintering processes on the mechanical properties and microstructure of Ti(C,N)-based cermet cutting tool materials, Int. J. Refract. Met. Hard Mater. 47 (2014) 71—79.

[26] A.P. Serro, C. Completo, R. Colaco, F. Dos Santos, C.L. Da Silva, J.M.S. Cabral, H. Araujo, E. Pires, B. Saramago, A comparative study of titanium nitrides, TiN, TiNbN and TiCN, as coatings for biomedical applications, Surf. Coat. Technol. 203 (2009) 3701—3707.

[27] P. Li, J. Ye, Y. Liu, D. Yang, H. Yu, Study on the formation of core—rim structure in Ti(CN)-based cermets, Int. J. Refract. Met. Hard Mater. 35 (2012) 27—31.

[28] S. Ahn, S. Kang, Formation of core/rim structures in Ti(C,N)-WC-Ni cermets via a dissolution and precipitation process, J. Am. Ceram. Soc. 83 (2000) 1489—1494.

[29] T. Chartier, D. Merle, J.L. Besson, Laminar ceramic composites, J. Eur. Ceram. Soc. 15 (1995) 101—107.

[30] W. Lengauer, K. Dreyer, Functionally graded hardmetals, J. Alloy Compd. 338 (2002) 194—212.

[31] L. Li, L. Cheng, S. Fan, Y. Xie, J. Xue, L. Zhang, Effect of large thicknesses on the characteristics of laminated ZrO—Zr$_2$CN/Si$_3$N$_4$ ceramics by reactive hot pressing, J. Alloy Compd. 656 (2016) 654—662.